TÜBİTAK

Turkish Journal of Chemistry

http://journals.tubitak.gov.tr/chem/

Research Article

Turk J Chem
(2018) 42: 684 – 693

doi:10.3906/kim-1612-21

Highly efficient catalytic degradation of low-density polyethylene Using a novel tungstophosphoric acid/kaolin clay composite catalyst

Saira ATTIQUE[1], Madeeha BATOOL[1], Muhammad Irfan JALEES[2], Khurram SHEHZAD[3], Umar FAROOQ[2], Zakir KHAN[4], Fawad ASHRAF[4], Asma Tufail SHAH[5,*]

[1]Institute of Chemistry, University of the Punjab, Lahore, Pakistan
[2]Institute of Environmental Engineering and Research, University of Engineering and Technology, Lahore, Pakistan
[3]College of Information Science and Electronic Engineering and State Key Laboratory of Silicon Materials, Zhejiang University, Hangzhou, Zhejiang, P.R. China
[4]Department of Chemical Engineering, COMSATS University Islamabad, Lahore Campus, Lahore, Pakistan
[5]Interdisciplinary Research Centre in Biomedical Materials, COMSATS University Islamabad, Lahore Campus, Lahore, Pakistan

Received: 12.12.2016 • **Accepted/Published Online:** 01.02.2018 • **Final Version:** 01.06.2018

Abstract: In order to take advantage of the Brønsted acidity of tungstophosphoric acid (TPA) and Lewis acidity of kaolin, TPA-loaded kaolin catalysts with varying percentages of TPA (10–50 wt.-%) were prepared by wet impregnation method. Fourier transform infrared spectrometer, X-ray diffractometer, Brunauer–Emmett–Teller surface area analyzer, and scanning electron microscope characterizations were performed to confirm the successful loading of TPA on kaolin. Catalytic cracking of low-density polyethylene (LDPE), by employing TPA-loaded kaolin as the catalyst, produced a higher percentage of fuel oil (liquid and gaseous hydrocarbons) with a negligible amount of semisolid wax (1.0 wt.-%). The wax amount was significantly lower compared to the thermal cracking, which produced ∼22 wt.-% solid black residue. Moreover, GC-MS analysis of oil showed that thermal cracking produced mainly higher hydrocarbons (C_{22}) as compared to the catalytic cracking where larger fraction of lower hydrocarbons were obtained. We purpose that the higher performance of prepared catalysts was due to the presence of both Brønsted and Lewis acid sites, which increase their catalytic efficiency and degraded LDPE at the relatively lower temperatures. These results suggest that prepared materials were effective catalysts with low cost and easily scalable production method, suitable for large-scale high performance catalytic cracking of polymers.

Key words: Catalytic cracking, tungstophosphoric acid, polyethylene, kaolin

1. Introduction

Plastic waste represents an emergent social problem as it causes loss of natural resources and increase in environmental pollution. Landfilling, incineration, and thermal or catalytic degradation are important methods to dispose of plastic waste.[1−4] Landfilling seems to be ineffective, because large amounts of plastic materials require a large dumping area. Conversion of waste polymers to useful fuels by thermal or catalytic processes may be a promising solution that not only avoids the environmental hazards posed by these polymers, but also employs an attractive alternative source of energy production.[5−7] Catalytic degradation of waste polymers has considerable advantages over thermal degradation. For example, thermal processes require high temperature,

*Correspondence: drasmashah@ciitlahore.edu.pk

i.e. 500 °C– 900 °C, and produce a very broad product range.[8,9] On the other hand, use of catalyst not only reduces the reaction temperature[10] but also yields the liquid hydrocarbons that avoids the need for extra processing steps.[11]

The most commonly used catalysts for catalytic degradation of plastic waste (polymers) include zeolites,[12] solid silica-alumina,[13] activated carbon,[14] mesoporous materials,[15] polyoxometalates,[16] kaolin,[17] etc. Zeolites have excellent catalytic properties for degradation of polymers due to their strong acidity for carbon–carbon bond breakage. However, these catalysts have small pore size, which hinders the contact of bulky molecules to acid sites located inside the pores.[18] Therefore, mesoporous materials with large pore size were developed[19] but the catalytic use of mesoporous materials in pure silica form is limited due to their relatively low acidity, compared to those of microporous zeolites (HZSM-5, US-Y).[18] Polyoxometalates (POMs) are discrete multitransition metal oxides with strong Brønsted acid sites, which make them outstanding catalysts. However, there are very few studies in the literature that use heteropoly acids (HPAs) as the solid acid catalysts in polymer cracking reactions due to their low thermal stability and surface area.[15,16] In order to improve the catalytic performance of these materials, POMs have been incorporated into the silica framework.[20] The role of tungstophosphoric acid (TPA) supported on MCM-41 and SBA-15 has been investigated for the degradation of polyethylene.[10,20] In the presence of TPA-loaded silica material, activation energy can be reduced to half of the value compared to thermal degradation.[20]

Kaolin, a clay material used for degradation of polypropylene, offers advantages such as low cost and high thermal stability; however, its weak Lewis acidity and high degradation temperature (up to 500 °C)[17] prevent its widespread application. TPA, with excellent catalytic performance, due to the strong Brønsted acid sites, can be supported on the surface of kaolin to enhance its acidity.[21] With aim to obtain a low-cost, high performance catalyst for LDPE degradation, herein, we report a hybrid kaolin/TPA that combines the properties of both the materials for the low temperature (330 °C) degradation of polyethylene with high performance (low residue percentage, and olefin/paraffin ratio).

2. Results and discussion

2.1. Characterization of catalyst

In order to investigate the structural integrity of TPA, its final structural properties, and the morphological properties after loading, different analytical techniques were used. The type of functional groups was studied by FTIR spectroscopy. Figure 1a shows the FTIR spectra of kaolin, TPA, and TPA loaded on kaolin (1-TPA-K, 3-TPA-K, 5-TPA-K). In the FTIR spectrum of kaolin, absorptions at 761 cm^{-1} and 795 cm^{-1} are attributed to Si–O–Al vibrations and the band at 914 cm^{-1} is assigned to OH bending vibrations. The peak at 1007 cm^{-1} is assigned to Si–O–Si in-plane vibrations and at 1123 cm^{-1} is assigned to asymmetric Si–O–Si stretching vibrations.[22] The spectrum of pure TPA showed characteristic asymmetric vibrations for P–O_a–W (1084 cm^{-1}), W=O_d terminal (982 cm^{-1}), W–O_b –W interbridges between corner-sharing, WO_6 octahedra (895 cm^{-1}), and W–Oc–W interbridges between edge-sharing WO_6 octahedra (789 cm^{-1}).[23,24] The spectrum of TPA/kaolin with different percentages of TPA showed two bands of TPA at 991 and 923 cm^{-1}, which might be attributed to the W=O_d and W–O_b–W, respectively. However, the bands at 1084 and 789 cm^{-1} were not prominent due to overlapping with the strong bands of silica in the kaolin support.[21]

Figure 1b shows the XRD patterns. They show that kaolin is a highly crystalline material having char-

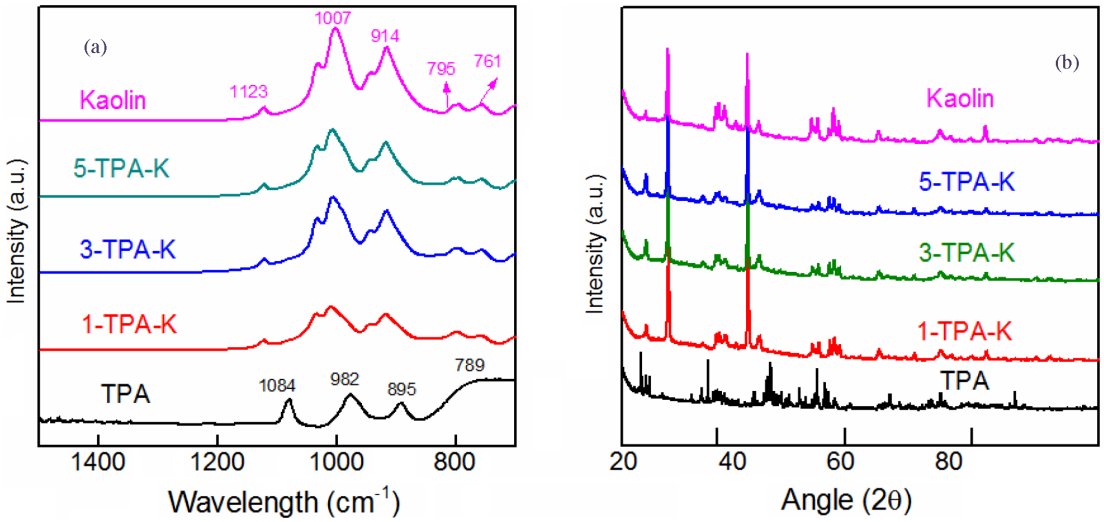

Figure 1. (a) FTIR spectrum, (b) XRD patterns of kaolin, TPA, 1-TPA-K, 3-TPA-K, and 5-TPA-K samples.

acteristic intense and narrow diffraction peak d(001) at 2ϑ value 12.32°.[21] Bulk TPA had all the characteristic peaks of TPA with a kegging structure.[25] At 10% TPA loading, the characteristic peak of TPA at $2\vartheta = 8.8°$ was very small and the intensity increased with TPA loading.[26] However, all the typical characteristic diffraction peaks of the crystalline phase of TPA were not observed, even for the 5-TPA-K sample, as compared to the XRD pattern of bulk TPA. This indicated that TPA was finely dispersed on the surface of kaolin.[27]

The surface area of kaolin is comparatively low; however, it has a number of Lewis acid sites. The BET surface area of the kaolin, TPA, and TPA loaded on kaolin were low (about 30–50 $m^2\ g^{-1}$). Thus the increase in catalytic activity was attributed to the acidic sites present in kaolin. The use of kaolin increases the thermal stability of TPA. Figure 2a shows the SEM micrograph of bulk TPA with well-shaped crystalline particles. Crystal size of TPA on average was 1 μm. Figure 2b presents the SEM image of 50 wt.-% TPA loaded on kaolin. Kaolin has a bulk crystalline structure on which TPA crystals were dispersed during impregnation. The micrographs show that TPA crystals were uniformly distributed on the kaolin surface.

2.2. Thermal catalytic cracking of low density polyethylene (LDPE)

It is well known that acidic catalysts lower the degradation temperature of polyethylene and improve the yield of hydrocarbons. The degradation temperature of polyethylene depends upon the nature of the catalyst.[28–30] Table 1 shows that the thermal pyrolysis/cracking of LDPE took place at 375 °C, while all catalysts lowered the degradation temperature of polymer below 340 °C. TPA, when used alone, degraded LDPE at further lower temperature (335 °C) and produced liquid hydrocarbons with relatively broad distribution and a significant amount of kerosene-like fractions (C_{11}–C_{17}). TPA-modified kaolin also degraded the polymer at 335 °C; however, it further enhanced liquid yield with predominant amounts of lower hydrocarbons (discussed in section 2.3).

2.3. Percentage yield of degradation products

Table 1 shows the percentage yield of different fractions obtained by the thermal and catalytic degradation of LDPE. Both oil and gas fractions of catalytic cracking are useful products.[31] The percentage yield of liquid and

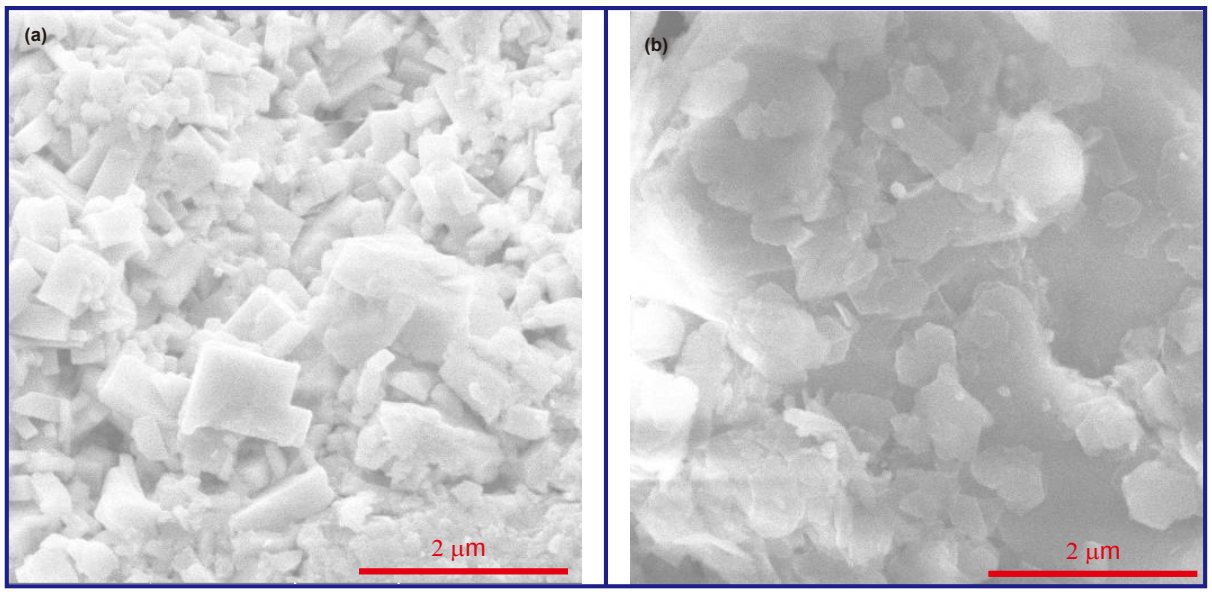

Figure 2. SEM micrographs of (a) bulk TPA, (b) 5-TPA-K.

Table 1. Percentage yield of different fractions formed during thermal and catalytic degradation of LDPE.

Catalyst	Cracking temperature (°C)	Reaction time (h)	Oil yield (%)	Gas (%)	Residue (%)
No catalyst	375	3.40	68	8	22
TPA	335	3.20	73.5	18	8.5
Kaolin	340	3.0	76	19.5	4.5
1-TPA/K	340	2.5	78	18.5	3.5
3-TPA/K	340	2.45	78.6	18.1	3.0
5-TPA/K	335	2.45	81	18	1.0

gas fractions obtained by cracking of polymer over different catalysts was higher compared to the noncatalytic degradation of polyethylene. TPA loaded on the kaolin surface showed a relatively high percentage of liquid yield. With an increase in TPA loading, the yield of fuel oil increased to 99 wt.-% (50% TPA loaded kaolin sample) with a residue of about 1 wt.%. Thermal pyrolysis produced only 68% liquid oil with 22% residue. The reason for the increase in yield was the combined effect of the Lewis acidity of kaolin and strong Brønsted acid sites on TPA.[21] Gaca et al.[28] also reported that TPA loaded on MCM-41 used for PE degradation resulted in specifically higher amounts of liquid products. The percentage yield of gaseous fractions (C_1–C_4) was higher for all catalysts compared to the noncatalytic degradation of polymer. Thus use of catalysts not only decreased the decomposition temperature but also increased the percentage yield of useful fuel products. Jalil[20] has also reported that use of TPA loaded on MCM-41 increased both liquid and gaseous products.

2.4. Composition of liquid product

The liquid oil obtained was subjected to GC-MS analysis. The main components obtained were olefin and paraffin (C_9–C_{26}). The details of compounds and their relative abundance are given in Table 2 and Figure

3. Liquid products received as a result of LDPE degradation contained both alkanes and alkenes. The ratio of alkenes and alkanes varied from 1:2 to 2:3, respectively. Table 2 indicates the relative abundance of alkanes and alkenes formed during the thermal and catalytic degradation of LDPE. Thermal degradation of LDPE produced aliphatic hydrocarbons approximately 1/3 of aliphatic hydrocarbons produced by TPA loaded with kaolin, while TPA and kaolin produced considerable amounts of hydrocarbons (Table 2). The same trend was observed in earlier reports.[32–34]

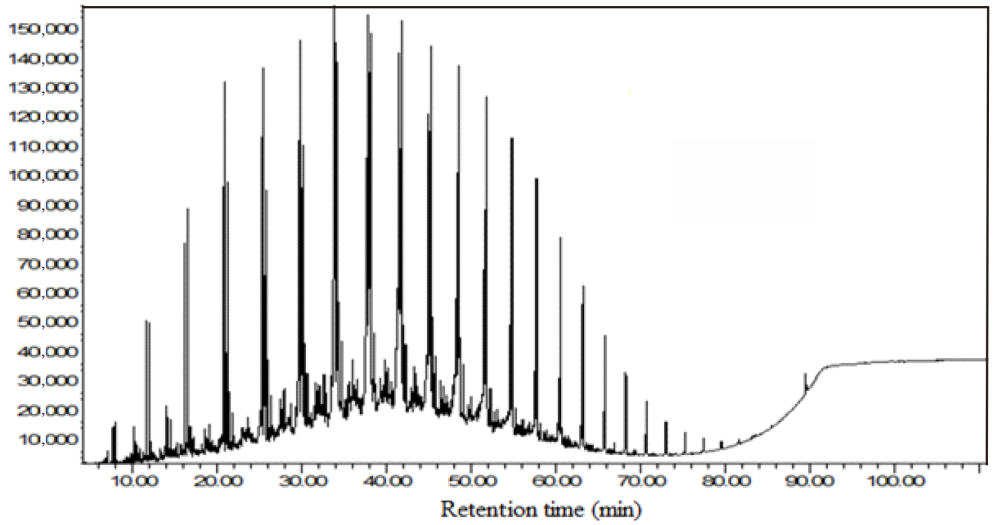

Figure 3. GC-MS of liquid products obtained by 5-TPA-K. The percentages of various peaks/compounds are given in Table 2.

The production of alkanes by thermal and catalytic cracking of LDPE is given in Figure 4. The cracking LDPE in the absence of catalyst produced very low quantity of alkanes, whereas kaolin and TPA produced higher quantity especially high molecular weight hydrocarbons in the range of C_{11}–C_{17} and C_{13}–C_{22}, respectively. Cracking over TPA loaded on kaolin (5-TPA-K) produced higher percentages of gasoline-like hydrocarbons (C_{11}–C_{14}), while a smaller amount of kerosene was produced. This might be due to the fact that TPA loading on kaolin will produce additional Brønsted acid sites with a positive effect on the catalyst activity for polymer degradation. The increase in the total acidity (Brønsted and Lewis) reduced the cracking temperature and led to degradation of heavier hydrocarbons to lighter ones due to the initiation of the LDPE degradation reaction proceeding over Brønsted acidic sites, as reported earlier by Aydemir et al.[31]

The quantity of alkenes produced was lower than that of the alkanes because high temperature favors the alkanes.[35] The Haag–Dessau mechanism explains the production of alkenes after thermal and catalytic cracking.[36] Many researchers explained the effect of Si/Al on the production of alkenes.[32–34] The quantity of alkenes produced was maximum in TPA-K due to Brønsted acidic sites and introduction of Si and Al in catalyst. The same effect was also observed in kaolin, where the production of alkenes was greater without catalyst (Figure 5).

2.5. Mechanism of polyethylene degradation

According to Choomwattana et al., POMs have a large number of protonic acid sites, which increase its catalytic activity many times for polymer cracking.[37] As TPA-K has both Brønsted and Lewis acid sites, it

Table 2. Identification of various aliphatic hydrocarbons produced using different catalysts.

RT (min)	Peak name	Relative abundance (%)			
		5-TPA-K	Kaolin	TPA	No catalyst
11.614	1-C9 (ene)	0.81	0.53	—	—
11.992	n-C9 (ane)	0.80	0.39	—	—
16.154	1-C10 (ene)	1.83	1.24	—	0.94
16.564	n-C10 (ane)	2.01	0.86	0.63	0.29
20.824	1-C11 (ene)	4.36	2.93	0.39	0.93
21.233	n-C11 (ane)	2.90	2.09	0.56	0.99
25.385	1-C12 (ene)	5.61	4.80	1.21	—
25.773	n-C12 (ane)	5.55	4.67	1.38	0.88
29.753	1-C13 (ene)	6.45	5.62	3.40	0.84
30.108	n-C13 (ane)	6.02	5.82	4.54	—
33.872	1-C14 (ene)	6.43	4.40	5.13	0.70
34.206	n-C14 (ane)	8.06	6.13	7.75	0.95
41.464	1-C15 (ene)	6.30	5.12	5.27	1.60
41.766	n-C15 (ane)	10.86	6.16	8.98	1.11
44.969	1-C16 (ene)	4.17	3.53	3.68	1.15
45.26	n-C16 (ane)	9.57	5.14	7.86	1.71
48.312	1-C17 (ene)	2.98	1.96	2.43	1.21
48.592	n-C17 (ane)	9.25	4.18	7.00	3.17
51.504	1-C18 (ene)	2.12	1.36	1.61	—
51.773	1-C18 (ane)	6.84	3.44	5.58	—
54.555	1-C19 (ene)	1.82	0.80	1.03	0.97
54.803	n-C19 (ane)	6.14	2.41	4.14	0.77
57.499	1-C20 (ene)	0.96	0.53	0.55	—
57.715	n-C20 (ane)	3.32	1.81	2.26	1.62
60.303	1-C21 (ene)	0.56	0.29	0.39	1.67
60.508	n-C21 (ane)	2.77	1.25	1.40	1.22
63.193	1-C22 (ane)	1.84	0.29	1.18	0.78
65.781	1-C23 (ane)	1.56	1.09	0.55	0.44
68.262	1-C24 (ane)	1.15	0.57	0.42	—
70.677	1-C25 (ane)	0.86	0.39	0.21	—
73.006	1-C26 (ane)	0.24	—	—	—

degraded polyethylene through an ionic mechanism and Lewis acid sites abstracted hydride ions from saturated hydrocarbons forming a carbenium ion, while Brønsted acid sites of catalyst added protons to olefins to form a carbocation.

In conclusion, TPA loaded on kaolin, for cracking of LDPE, significantly enhanced the yield of fuel oil (liquid and gaseous hydrocarbons), as TPA-impregnated kaolin samples were active for conversion of LDPE to lower hydrocarbons. With the increase in TPA loading, oil yield was increased, and the highest oil yield was

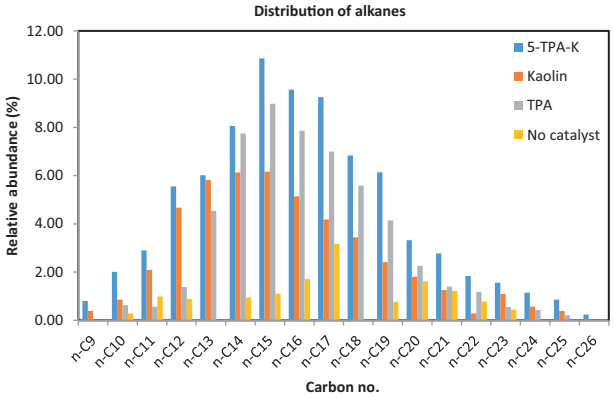

Figure 4. Percentage relative abundance of alkanes obtained by thermal and catalytic cracking of LDPE.

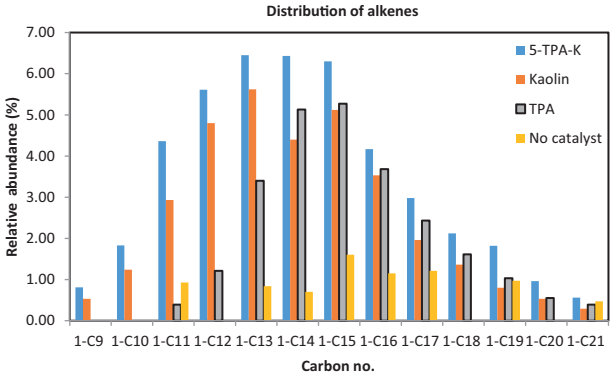

Figure 5. Relative abundance of alkenes obtained from thermal and catalytic cracking of LDPE.

obtained for the maximum loading of TPA investigated in this study (5-TPA-K sample). Cracking temperature of LDPE also shifted to a lower value in the presence of these catalysts, lowering the overall cost of the process by saving energy. Valuable petrochemicals were recovered from plastic waste using these catalysts, which suggest the application of our catalyst for effective pollution control and energy production from the waste.

3. Experimental

3.1. Materials

Disodium hydrogen phosphate ($Na_2HPO_4.12H_2O$) 98%; Sigma Aldrich. Sodium tungstate dehydrate ($Na_2WO_4.2H_2O$); Merck. Hydrochloric acid; Green chemicals. Low density polyethylene pellets (melting point range 140–150 °C); Qatar Chemical and Petrochemical Marketing and Distribution Company.

3.2. Synthesis of catalysts

3.2.1. Synthesis of tungstophosphoric acid (TPA)

In a typical synthetic procedure 15.1 mmol of sodium tungstate (5 g) and 2.5 mmol of sodium hydrogen phosphate (0.45 g) were dissolved in 20 mL of H_2O to yield a transparent solution as reported by Dong et al.[38] Hydrochloric acid (HCl) solution (4 M) was added dropwise to adjust the pH value to 1.0–2.0 and reacted for 2 h at 75 °C. Then 10 mL of HCl solution was added while stirring. When half of the acid has been added, TPA begins to separate. After cooling to room temperature, the solution was extracted with diethyl ether. The oil-like organic layer was evaporated at room temperature to form crystals.

3.2.2. Preparation of TPA-loaded kaolin catalyst (TPA-K)

Kaolin clay (1 g) was dispersed in water (50 mL) by stirring for 4 h. TPA, dissolved in a minimal amount of water, was added slowly to the clay dispersion (0.1, 0.3, and 0.5 g to prepare 10%, 30%, and 50% TPA/K samples). The reaction mixture was stirred for 12 h at room temperature. Then the water was removed by heating at 60 °C on a water bath. The samples were dried overnight in an oven at 110 °C. The prepared samples were designated as 1-TPA-K, 3-TPA-K, and 5-TPA-K designating 10%, 30%, and 50% POM loaded on kaolin.

3.3. Thermal and catalytic cracking of LDPE

Cracking of LDPE was carried out in a glass reactor (5-cm id, 25-cm length) by batch operation. Figure 6 shows the schematic representation of experimental setup. First, 15 g of polyethylene pellets mixed with 0.75 g catalyst (5 wt.-%) was loaded into the reactor for catalytic cracking. After the reactor was set up, nitrogen was purged into the reactor to remove air and water vapors. The reactor was then heated to 140 °C at a heating rate of 2 °C min^{-1} and held at 140 °C for 1 h to evaporate adsorbed water. The nitrogen supply was cut off and temperature was raised to cracking temperature at a heating rate of 5 °C min^{-1}. The degradation products were classified into three groups: gases (products that were not condensable at water cooling temperature), liquid hydrocarbons, and residues. The experimental run was finished when no oil drop came out for at least 30 min. The amount of gaseous products was estimated by subtracting the weight of liquid products and residues from the plastic sample feed. The term residue refers to both the carbonaceous and the waxy compounds remaining in the reactor after the degradation reaction. Liquid products were analyzed by GC-MS.

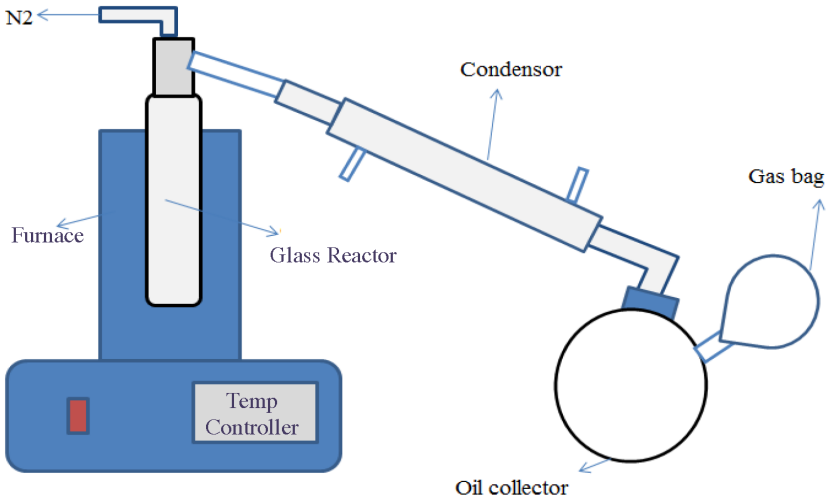

Figure 6. Schematic diagram of the set up used for thermal and catalytic cracking of polymer.

3.4. Characterization techniques

The prepared catalysts were characterized by different qualitative techniques to evaluate their physical properties and structural integrity after TPA loading. A Fourier transform infrared spectrometer (FTIR) (Agilent technology model 41630) (ATR mode) was used to investigate the structural changes in prepared samples. Spectra were obtained at 4 cm^{-1} resolution, accumulating 256 number of scans within mid-IR range (4000–400 cm^{-1}). The crystalline structure of catalysts was determined by X-ray diffractometer (XRD) from PANalytical (XPERT-PRO model) operated at 40 kV and 40 mA using Cu Kα radiation. The detector was scanned over a range of angle 2θ =10°–60° at a step size of 0.02°. Brunauer–Emmett–Teller (BET) surface area was measured by nitrogen gas adsorption/desorption method using a Micromeritics' New TriStar II Surface Area analyzer. Before analysis, the samples were degassed at 200 °C with a heating ramp of 10 °C/min for 4 h in a nitrogen environment. The morphology was studied using a TESCAN Vega3 LMU scanning electron microscope (SEM). The samples were precoated using gold targets for 90 s using a sputter coater from Quorum Technologies.

4. Acknowledgments

We are grateful to the International Foundation of Science (IFS) for fully funding this project for performing the experiments by grant (F/5375-1). The Ministry of Science and Technology (MOST) and Higher Education Commission, Pakistan, are thanked for developmental grants.

References

1. Serrano, D. P.; Aguado, J.; Escola, J. M. *ACS Catal.* **2012**, *2*, 1924-1941.
2. Aguado, J.; Serrano D. P.; Escola, J. M. *Ind. Eng. Chem. Res.* **2008**, *47*, 7982-7992.
3. Lee, J. Y.; Park, S. M.; Saha S. K.; Cho, S. J.; Seo, G. *Appl. Catal. B: Environ.* **2011**, *108*, 61-71.
4. Serrano, D. P.; Aguado, J.; Escola, J. M.; Rodríguez, J. M.; Peral, Á. *Chem. Mater.* **2006**, *18*, 2462-2464.
5. Brandrup, J.; Bittner, M.; Michaeli, W.; Menges, G. *Recycling and Recovery of Plastics*; Hanser: Munich, Germany, 1996.
6. Scott, G.; Billingham, N.; *Polymers and the Environment*; The Royal Society of Chemistry: Cambridge, UK, 1999.
7. Sarker, M.; Rashid, M. M.; Molla, M.; Sadikur Rahman, M. *Int. J. Energy Environ.* **2012**, *3*, 749-760.
8. Akpanudoh, N. S.; Gobin, K.; Manos, G. *J. Mol. Catal. A-Chem.* **2005**, *235*, 67-73.
9. Lin, Y. H.; Yang, M. H.; Yeh, T. F.; Ger, M. D. *Polym. Degrad. Stabil.* **2004**, *86*, 121-128.
10. Abdalla, Z. E. A.; Li, B.; Tufail, A. *Ind. Eng. Chem. Res.* **2011**, *15*, 780-783.
11. Kim, J. R.; Kim, Y. A.; Yoon, J. H.; Park, D. W.; Woo H. C. *Polym. Degrad. Stabil.* **2002**, *75*, 287-294.
12. Kaminsky, W.; Zorriqueta, I. J. N. *J. Anal. Appl. Pyrolysis* **2007**, *79*, 368-374.
13. Aguado, J.; Sotelo, J. L.; Serrano, D. P.; Calles, J.A.; Escola, J. M. *Energy Fuels* **1997**, *11*, 1225-1231.
14. Uemichi, Y.; Makino, Y.; Kanazuka, T. *J. Anal. Appl. Pyrolysis* **1989**, *16*, 229-238.
15. Ghanbari-Siahkali, A.; Philippou, A.; Garforth, A.; Cundy, C. S.; Anderson, M. W.; Dwyer, J. *J. Mater Chem.* **2001**, *11*, 569-577.
16. Thomas, A.; Dablemont, C.; Basset, J. M.; Lefebvre, F. *Comptes Rendus Chimie* **2005**, *8*, 1969-1974.
17. Panda, A. K.; Singh, R. *Adv. Energy Eng.* **2013**, *1*, 74-84.
18. Marcilla, A.; Gomez-Siurana, A.; Berenguer, D. *Appl. Catal. A - General* **2006**, *301*, 222-231.
19. Kresge, C. T.; Leonowicz, M.; Roth, W.; Vartuli J. C.; Beck, J. S. *Nature* **1992**, *359*, 710-712.
20. Jalil, P.A. *J. Anal. Appl. Pyrolysis* **2002**, *65*, 185-195.
21. Basira, N. M.; Lintang, H. O.; Endud, S. *J. Teknologi.* **2015**, *76*, 27-34.
22. Kuang, W.; Rives, A.; Fournier, M.; Hubaut, R. *Appl. Catal. A - General* **2003**, *250*, 221-229.
23. Rocchiccioli-Deltcheff, C.; Fournier, M.; Franck, R.; Thouvenot, R. *Inorg. Chem.* **1983**, *22*, 207-216.
24. Shah, A. T.; Mujahid, A.; Farooq, M. U.; Ahmad, W.; Li, B.; Irfan, M.; Qadir, M. A. *J. Sol-Gel Sci. Technol.* **2012**, *63*, 194-199.
25. Wang, W.; Yang, S. *J. Water Resource and Protection* **2010**, *2*, 979-983.
26. Aydemir, B.; Aslı-Sezgi, N.; Doğu, T. *AIChE J.* **2012**, *58*, 2466-2472.
27. Dong, B. B.; Zhang, B. B.; Wu, H. Y.; Chen, X.; Zhang, K.; Zheng, X. C. *Mater. Res. Bull.* **2013**, *48*, 2491-2496.
28. Gaca, P.; Drzewiecka, M.; Kaleta, W.; Kozubek, H.; Nowinska, K. *Polish J. Environ. Stud.* **2008**, *17*, 25-31.
29. Chandrasekaran, S. R.; Kunwar, B.; Moser, B. R.; Rajagopalan N.; Sharma, B. K. *Energy Fuels* **2015**, *29*, 6068-6077.

30. Azhar-Uddin, M.; Sakata, Y.; Muto, A.; Shiraga, Y.; Koizumi, K.; Kanada, Y.; Murata, K. *Microporous Mesoporous Mat.* **1998**, *21*, 557-564.

31. Aydemir, B.; Sezgi, N. A. *Ind. Eng. Chem. Res.* **2013**, *52*, 15366-15371.

32. Yoshimura, Y.; Kijima, N.; Hayakawa, T.; Murata, K.; Suzuki, K.; Mizukami, F.; Matano, K.; Konishi, T.; Oikawa, T.; Saito, M. *Catal. Surv. Jpn.* **2001**, *4*, 157-167.

33. Wei, Y.; Liu, Z.; Wang, G.; Qi, Y.; Xu, L.; Xie, P.; He, Y. *Stud. Surf. Sci. Catal.* **2005**, *158*, 1223-1230.

34. Corma, A.; Corresa, E.; Mathieu, Y.; Sauvanaud, L.; Al-Bogami, S.; Bourane, A. *Catal. Sci. Technol.* **2017**, *7*, 12-46.

35. Rahimi, N.; Karimzadeh, R. *Appl. Catal. A- General* **2011**, *398*, 1-17.

36. Kotrel, S.; Knözinger, H.; Gates, B. *Microporous Mesoporous Mat.* **2000**, *35*, 11-20.

37. Choomwattana, S.; Maihom, T.; Boekfa, B.; Pantu, P.; Limtrakul, J. *Can. J. Chem. Eng.* **2012**, *90*, 865-872.

38. Dong, B. B.; Zhang, B. B; Wu, H. Y.; Li, S. D.; Zhang, K.; Zheng, X. C. *Microporous Mesoporous Mat.* **2013**, *176*, 186-193.